Journal of Sound and Vibration 330 (2011) 1211–1224

Contents lists available at ScienceDirect

Journal of Sound and Vibration

journal homepage: www.elsevier.com/locate/jsvi

Propagation of uncertainty in test-analysis correlation of substructured spacecraft

Daniel C. Kammer*, Sonny Nimityongskul

Department of Engineering Physics, University of Wisconsin, 1500 Engineering Dr., Madison, WI 53706, USA

ARTICLE INFO

Article history:
Received 23 February 2010
Received in revised form
7 September 2010
Accepted 24 September 2010
Handling Editor: S. Ilanko
Available online 20 October 2010

ABSTRACT

Organizations, such as the Air Force and NASA make critical decisions on spacecraft performance and survivability based on the results of test-analysis correlation metrics. In order to ensure the success of a new paradigm in finite element model validation where there is no system level test, uncertainty in the substructures must be propagated into the system level correlation metrics. The objective of this work is to quantify the level of accuracy required at the substructure level to produce acceptable analytical model accuracy at the system level. In preparation for future synthesized system level uncertainty analysis, a framework is presented for propagating analytical model uncertainty from a fixed interface Craig–Bampton substructure representation into a free–free substructure. Model uncertainty is parameterized in terms of test- or truth-analysis correlation metrics that are dictated by the Air Force. A statistical model is presented for these correlation metrics such that an analyst can specify a covariance matrix for uncertainty in model correlation at the fixed substructure level, and then propagate it into correlation uncertainty at the free substructure level. Development of the forward propagation approach then allows propagation of correlation uncertainty in the reverse direction from the free substructure into the fixed interface based Craig–Bampton representation. The proposed methods are applied to a typical spacecraft representation.

1. Introduction

The aerospace community has long relied on modal analysis and the finite element method to perform linear dynamic predictions of spacecraft response. In the low frequency range, a relatively small number of modes can be used to capture the system behavior. Prior to flight, a test-validated finite element model (FEM) of the spacecraft must be developed to provide accurate loads analysis. The FEM validation process is comprised of several activities, such as determining the fidelity of the model to test data, quantification of uncertainty, and determining predictive accuracy [1–3]. Determining the fidelity-to-data is an exercise of fundamental importance. It is the process of comparing test and analysis predictions, also called test-analysis correlation, and then determining optimum changes in parameters that will update, calibrate, or tune the model [4]. In modal based validation, the accuracy of the FEM is determined by comparing test and analysis modal parameters. Frequencies are compared directly, while the corresponding mode shapes are compared using metrics based on orthogonality and cross-orthogonality of the modes with respect to a reduced analytical mass matrix [5]. The use of these metrics, and the required values for test-analysis correlation, are dictated by agencies such as NASA [6] and the United States Air Force. The requirements differ, depending on the agency. For example, the Air Force requires test-analysis

* Corresponding author. Tel.: +1 608 262 5724.
E-mail addresses: kammer@engr.wisc.edu, dckammer@facstaff.wisc.edu (D.C. Kammer).

0022-460X/$ - see front matter © 2010 Elsevier Ltd. All rights reserved.
doi:10.1016/j.jsv.2010.09.029

frequency errors less than or equal to 3.0%, cross-generalized mass values greater than 0.95, and coupling terms between modes of less than 0.10 in both cross-orthogonality and orthogonality [7].

Over the last decade, work in the structural dynamics community on analytical model validation has focused on the quantification of model uncertainty within large numerical simulations, and its propagation into predicted results [8–10]. The concept of model uncertainty is the reality of the design problem. An engineer may design a single structure based on drawings, analysis, and experiments, but then the item produced is one of a statistical population due to variations and uncertainties in geometry, material parameters, construction, etc. This leads to random populations of frequencies and mode shapes. Obviously, there is a corresponding uncertainty and error in the measured test data. In the low frequency regime of modal-based test-analysis correlation and model updating, it is common practice to ignore the effects of both model and test uncertainty. If one does not examine the agreement between measurements and predictions relative to uncertainty, very erroneous and dangerous decisions can be made regarding the models ability to make accurate predictions within untested regimes [11]. Hasselman and his coauthors have produced a large body of work [12–14] comparing several techniques for propagating uncertainty through structural dynamic simulations, such as linear covariance propagation, the Vertex Method for fuzzy variables, Monte Carlo analysis, etc.

As spacecraft become larger and more complex, ground based vibration tests of the entire structure become impossible due to lack of structural integrity, cost, complexity of the test, or simply lack of time. The spacecraft must then be validated on a substructure-by-substructure basis. Unavoidable uncertainty in substructure models and testing will have large, and possibly negative, impact on this new paradigm for model validation. Several critical questions must be addressed. What level of accuracy or correlation do the substructures need to exhibit, to have a required level of correlation at the system level? More specifically, how does uncertainty and error within a substructure propagate into, and affect model validation at the system level? Finally, how does uncertainty and error in the connections between substructures propagate into the system correlation? Even if the spacecraft will be tested as a system prior to launch, an understanding of the required level of substructure correlation, and how the related uncertainty propagates into the system, will save a great deal of time, effort, and cost during the system level test and analysis.

Recently, researchers have started to investigate the effects of substructure uncertainty on synthesized system response using component mode synthesis (CMS). The CMS approach has been used for years to solve large structural dynamics problems, and is built into many standard finite element analysis codes. Hinke et al. [15] consider uncertainty in the form of experimental measured variability, or noise, in substructure free–free modes. They use linear perturbation theory to determine the sensitivities of both fixed interface substructure, and global system modal parameters in terms of unconstrained substructure eigenvalues, based on the Craig–Bampton (CB) substructure representation [16]. Substructure eigenvalue variance is propagated into global statistics using linear covariance propagation. However, they only consider uncertainty in the substructure eigenvalues. De Klerk and Voormeeren [17] also consider substructure uncertainty in the form of experimental noise, but instead, it is in the frequency response measured during the substructure vibration test. They use a frequency domain CMS approach. Linear perturbation theory is used to propagate the substructure uncertainty into the global response. Neither of these investigations considered uncertainty in model form.

Babuska et al. [18] address substructure model uncertainty in the form of physical parameter or component modal perturbations. They propagate substructure uncertainty into system frequency response using Linear Fractional Transformations and system level Monte Carlo analysis. The approach can result in large matrices and large computation cost. Its focus is more on control dynamics applications rather than structural dynamics. Mace and Shorter [19] also consider the effects of substructure model uncertainty on the system modal parameters and frequency response. They use the CB formulation and linear perturbation theory to determine system modal parameters in terms of the random substructure modal parameters. Uncertainty in the substructure modal parameters is propagated into system modal parameters using a decoupled Monte Carlo approach. Uncertainty in the system level frequency response can then also be determined. None of the work performed in this area addresses the test-analysis correlation component of model validation, at either the substructure or system level.

The goal of this investigation is to develop a methodology for studying the effects of uncertainty on metrics used for test-analysis correlation of complex spacecraft that are validated on a substructure-by-substructure basis. The objective is to quantify the level of accuracy required at the substructure level to produce acceptable accuracy at the system level. In preparation for future synthesized system level uncertainty analysis, this paper will first present uncertainty propagation at the substructure level. Linear perturbation analysis is used to relate uncertainty in test-analysis correlation metrics to uncertainty in substructure modal mass and stiffness. A statistical model for modal based test-analysis correlation metrics is developed which results in an assumed covariance matrix. Linear covariance propagation is then used to propagate fixed-interface modal correlation metric uncertainty into the expected free–free substructure correlation metric uncertainty using a CB substructure representation. Reverse covariance propagation [12] is also investigated for the purpose of propagating from assumed free–free substructure metrics into the fixed substructure. This propagation direction can be more critical because substructure vibration tests are often conducted in a free–free configuration.

Organizations, such as NASA and the Air Force make critical decisions on spacecraft performance and survivability based on the results of test-analysis correlation metrics. Currently there is no uncertainty quantification performed or required by these agencies for test-analysis correlation in the low-frequency regime. The approach presented in this paper offers several advantages over other methods. A user can choose to propagate either an assumed level of test-analysis correlation uncertainty, or uncertainty derived from vibration test results. It is not reliant on any specific model design

parameters. It includes all forms of model uncertainty. It is fast, compared with Monte Carlo techniques, and it propagates uncertainty in the correlation metrics directly.

2. Theory

The CB substructure representation is well suited as a building block for model validation of a substructured system. In physical coordinates, the undamped equations of motion for the free–free substructure are given by

$$\mathbf{M}\ddot{\mathbf{u}}+\mathbf{K}\mathbf{u}=\begin{bmatrix}\mathbf{M}_{oo} & \mathbf{M}_{oa}\\ \mathbf{M}_{ao} & \mathbf{M}_{aa}\end{bmatrix}\begin{Bmatrix}\ddot{\mathbf{u}}_o\\ \ddot{\mathbf{u}}_a\end{Bmatrix}+\begin{bmatrix}\mathbf{K}_{oo} & \mathbf{K}_{oa}\\ \mathbf{K}_{ao} & \mathbf{K}_{aa}\end{bmatrix}\begin{Bmatrix}\mathbf{u}_o\\ \mathbf{u}_a\end{Bmatrix}=\begin{Bmatrix}\mathbf{0}\\ \mathbf{F}_a\end{Bmatrix} \tag{1}$$

where the a partitions correspond to degrees of freedom that interface to other substructures and the o partitions correspond to degrees of freedom that are interior to the substructure. The CB representation is generated using the coordinate transformation

$$\mathbf{u}=\begin{Bmatrix}\mathbf{u}_o\\ \mathbf{u}_a\end{Bmatrix}=\begin{bmatrix}\boldsymbol{\phi} & \boldsymbol{\psi}\\ \mathbf{0} & \mathbf{I}\end{bmatrix}\begin{Bmatrix}\mathbf{q}\\ \mathbf{u}_a\end{Bmatrix}=\mathbf{T}\mathbf{u}_{\mathrm{CB}} \tag{2}$$

in which $\mathbf{u}_a$ represents the displacement of the substructure interface, and $\mathbf{u}_o$ is the displacement of the interior of the substructure. This representation is characterized by a combination of fixed interface dynamic shapes, $\boldsymbol{\phi}$, and a set of static shapes, $\boldsymbol{\Psi}=[\boldsymbol{\psi}^{\mathrm{T}}\quad \mathbf{I}]^{\mathrm{T}}$, called constraint modes, in which $\boldsymbol{\psi}=-\mathbf{K}_{oo}^{-1}\mathbf{K}_{ao}$. The substructure mass and stiffness matrices in the CB space are then given by

$$\mathbf{M}_{\mathrm{CB}}=\mathbf{T}^{\mathrm{T}}\mathbf{M}\mathbf{T}=\begin{bmatrix}\mathbf{m} & \mathbf{M}_{qa}\\ \mathbf{M}_{aq} & \mathbf{M}_S\end{bmatrix}\quad \mathbf{K}_{\mathrm{CB}}=\mathbf{T}^{\mathrm{T}}\mathbf{K}\mathbf{T}=\begin{bmatrix}\mathbf{k} & \mathbf{0}\\ \mathbf{0} & \mathbf{K}_S\end{bmatrix} \tag{3}$$

where $\mathbf{m}$ and $\mathbf{k}$ are the fixed interface nominal modal mass and stiffness matrices, respectively, $\mathbf{M}_{qa}$ is the mass coupling between fixed modal degrees of freedom and the physical interface degrees of freedom, and $\mathbf{M}_S$ and $\mathbf{K}_S$ represent the substructure mass and stiffness matrices statically reduced to the interface, respectively.

If all of the fixed-interface modes are retained, then the transformation into the CB substructure representation is exact. However, a significant reduction in model size can be achieved by truncating the number of fixed-interface modes based on frequency. Eq. (3) provides a direct connection between substructure fixed-interface and free-interface modes through the fixed interface modal mass $\mathbf{m}$, and the modal stiffness $\mathbf{k}$. The efficacy of this substructure representation for studying the effects of model uncertainty lies in the fact that the interior and interface of the substructure are represented separately. Therefore, the effects of uncertainty from each source can be considered somewhat independently.

2.1. Linear perturbation analysis

The perturbation analysis presented in this paper follows that of Hasselman [20]. However, there are a few notable exceptions that will be discussed. Uncertainty in modal mass and stiffness will be linked to uncertainty in modal frequency and cross-orthogonality. While the presentation is specifically directed at a fixed interface substructure, the results are equally applicable to an unconstrained substructure. The uncertainty is defined with respect to the nominal substructure FEM. The nominal fixed interface modes are assumed to be normalized with respect to mass, such that $\mathbf{m}=\mathbf{I}$ and $\mathbf{k}=\boldsymbol{\Omega}$, where $\boldsymbol{\Omega}$ are the nominal eigenvalues. The "truth" model of the constrained substructure can also be represented in nominal modal coordinates as

$$\mathbf{m}_T=\boldsymbol{\phi}^{\mathrm{T}}\mathbf{M}_{Too}\boldsymbol{\phi} \tag{4}$$

$$\mathbf{k}_T=\boldsymbol{\phi}^{\mathrm{T}}\mathbf{K}_{Too}\boldsymbol{\phi} \tag{5}$$

in which $\mathbf{M}_{Too}$ and $\mathbf{K}_{Too}$ are the true mass and stiffness matrices, if they existed. The uncertainty in the modal mass and stiffness can then be defined as

$$\Delta\mathbf{m}=\mathbf{m}_T-\mathbf{m}=\mathbf{m}_T-\mathbf{I}\quad\text{and}\quad\Delta\mathbf{k}=\mathbf{k}_T-\mathbf{k}=\mathbf{k}_T-\boldsymbol{\Omega} \tag{6}$$

Uncertainty in fixed interface modes and eigenvalues can likewise be expressed as

$$\Delta\boldsymbol{\phi}=\boldsymbol{\phi}_T-\boldsymbol{\phi}\quad\text{and}\quad\Delta\boldsymbol{\Omega}=\boldsymbol{\Omega}_T-\boldsymbol{\Omega} \tag{7}$$

As in Hasselman [20], the truth modes, in general, can be written in the form

$$\boldsymbol{\phi}_T=\boldsymbol{\phi}\boldsymbol{\gamma}+\boldsymbol{\varepsilon} \tag{8}$$

The first term on the right represents a linear combination of the nominal modes, while ε is a linear combination of residual nominal modes. Obviously, if all of the fixed interface modes are retained, then $\varepsilon=0$. Cross-orthogonality between

the nominal and truth modes can be written as

$$\boldsymbol{\phi}^{\mathrm{T}}\mathbf{M}_{oo}\boldsymbol{\phi}_T = \boldsymbol{\phi}^{\mathrm{T}}\mathbf{M}_{oo}\boldsymbol{\phi}\boldsymbol{\gamma} + \boldsymbol{\phi}^{\mathrm{T}}\mathbf{M}_{oo}\boldsymbol{\varepsilon} \tag{9}$$

In contrast with Hasselman [20], here it is assumed that the truth modes, $\boldsymbol{\phi}_T$, are normalized with respect to the nominal mass matrix, instead of the unknown truth mass matrix. This is done to be consistent with the definitions of cross-orthogonality used by both the United States Air Force [7] and NASA [6]. Therefore, for the jth mode

$$\boldsymbol{\phi}_{Tj}^{\mathrm{T}}\mathbf{M}_{oo}\boldsymbol{\phi}_{Tj} = [\boldsymbol{\phi}\boldsymbol{\gamma}_{\mathrm{j}} + \varepsilon_j]^{\mathrm{T}}\mathbf{M}_{oo}[\boldsymbol{\phi}\boldsymbol{\gamma}_{\mathrm{j}} + \boldsymbol{\varepsilon}_j] = 1 \tag{10}$$

or

$$\boldsymbol{\gamma}_{\mathrm{j}}^{\mathrm{T}}\boldsymbol{\gamma}_{\mathrm{j}} + \boldsymbol{\varepsilon}_{\mathrm{j}}^{\mathrm{T}}\mathbf{M}_{\mathrm{oo}}\boldsymbol{\varepsilon}_{\mathrm{j}} = \boldsymbol{\gamma}_{\mathrm{j}}^{\mathrm{T}}\boldsymbol{\gamma}_{\mathrm{j}} + \boldsymbol{\beta}_{\mathrm{j}} = 1 \tag{11}$$

in which the subscript j indicates the corresponding matrix columns of $\boldsymbol{\gamma}$ and $\boldsymbol{\varepsilon}$. Consistent with linear perturbation theory, it is assumed that the nominal model is close to the truth. Therefore, as is customary, it will be assumed that $\boldsymbol{\varepsilon}$ is small in Eq. (8), so that $\boldsymbol{\phi}_T \approx \boldsymbol{\phi}\gamma$, $\Delta\boldsymbol{\phi} \approx \boldsymbol{\phi}\Delta\boldsymbol{\gamma}$, and the cross-orthogonality in Eq. (9) becomes $\boldsymbol{\gamma}$. Eq. (11) reduces to $\boldsymbol{\gamma}_{\mathrm{j}}^{\mathrm{T}}\boldsymbol{\gamma}_{\mathrm{j}} = 1$, and the value of β_j gives a measure of the error [20]. In an actual application of test-analysis correlation, the cross-orthogonality between test and FEM modes is calculated with respect to a reduced FEM mass matrix called a test-analysis model (TAM), instead of the full mass matrix $\mathbf{M}_{oo}$. However, if the truth modes are spanned by the nominal modes and an exact model reduction is used, such as the Modal TAM [21], then the cross-orthogonality results are the same.

Due to the constraint of unit length for each column of the cross-orthogonality matrix, the value of the cross-generalized mass matching the jth nominal FEM mode with the jth truth mode, γ_{jj}, must lie in the range $0 \le \gamma_{jj} \le 1$ after being normalized to a positive value. Uncertainty in the cross-orthogonality matrix, $\Delta\boldsymbol{\gamma}$, can be defined using the expression $\boldsymbol{\gamma}=\mathbf{I}+\Delta\boldsymbol{\gamma}$. The constraint on the jth column of $\boldsymbol{\gamma}$ can then be expressed as

$$\boldsymbol{\gamma}_{\mathrm{j}}^{\mathrm{T}}\boldsymbol{\gamma}_{\mathrm{j}} = (1 + \Delta\boldsymbol{\gamma}_{\mathrm{jj}})^2 + \sum_{\substack{\mathrm{i}=1 \\ \mathrm{i}\neq\mathrm{j}}}^{\mathrm{n_q}} \Delta\boldsymbol{\gamma}_{\mathrm{ij}}^2 = 1 \tag{12}$$

or

$$\sum_{i=1}^{n_q} \Delta\boldsymbol{\gamma}_{\mathrm{ij}}^2 = -2\Delta\boldsymbol{\gamma}_{\mathrm{jj}} \tag{13}$$

where n_q is the number of nominal FEM and truth modes being correlated. Eq. (13) indicates that the uncertainty $\Delta\gamma_{jj}$ is always negative, and within each column of the cross-orthogonality matrix $\boldsymbol{\gamma}$, there is a constraint between the diagonal term and the off-diagonal terms given by

$$\sum_{\substack{i=1 \\ i\neq j}}^{n_q} \Delta\boldsymbol{\gamma}_{\mathrm{ij}}^2 = 1 - \boldsymbol{\gamma}_{\mathrm{jj}}^2 = -\Delta\boldsymbol{\gamma}_{\mathrm{jj}}^2 - 2\Delta\boldsymbol{\gamma}_{\mathrm{jj}} \tag{14}$$

The goal of this presentation is to relate uncertainty in the correlation metrics $\Delta\boldsymbol{\gamma}$ and $\Delta\boldsymbol{\Omega}$ to uncertainty in the fixed substructure modal mass and stiffness $\Delta\mathbf{m}$ and $\Delta\mathbf{k}$. Using the fact that the nominal fixed modes are mass normalized, and the previous uncertainty definitions, the orthogonality of the truth modes with respect to the truth mass can be written in the form

$$\boldsymbol{\phi}_T^{\mathrm{T}}\mathbf{M}_{Too}\boldsymbol{\phi}_T = [\boldsymbol{\phi} + \Delta\boldsymbol{\phi}]^{\mathrm{T}}[\mathbf{M}_{oo} + \Delta\mathbf{M}_{oo}][\boldsymbol{\phi} + \Delta\boldsymbol{\phi}] = \mathbf{I} + \boldsymbol{\delta}_M + \Delta\mathbf{m} + \Delta\boldsymbol{\gamma}^{\mathrm{T}}\Delta\mathbf{m} + \Delta\mathbf{m}\Delta\boldsymbol{\gamma} + \Delta\boldsymbol{\gamma}^{\mathrm{T}}\Delta\mathbf{m}\Delta\boldsymbol{\gamma} \tag{15}$$

where

$$\boldsymbol{\delta}_M = \Delta\boldsymbol{\gamma} + \Delta\boldsymbol{\gamma}^{\mathrm{T}} + \Delta\boldsymbol{\gamma}^{\mathrm{T}}\Delta\boldsymbol{\gamma} \tag{16}$$

The left side of Eq. (15) can also be expressed as $\boldsymbol{\phi}_T^{\mathrm{T}}\mathbf{M}_{Too}\boldsymbol{\phi}_T = \mathbf{I} + \Delta_M$ where Δ_M is a diagonal matrix in which Δ_{Mjj} represents the uncertainty in the jth generalized mass with respect to the truth modal space. Combining this result with Eq. (15) and dropping second-order terms in uncertainty gives

$$\Delta\mathbf{m} = \Delta_M - \delta_M \tag{17}$$

The expression for $\boldsymbol{\delta}_M$ in Eq. (16) appears to have a second-order term in $\Delta\boldsymbol{\gamma}^{\mathrm{T}}\Delta\boldsymbol{\gamma}$. While the off-diagonal terms in $\Delta\boldsymbol{\gamma}^{\mathrm{T}}\Delta\boldsymbol{\gamma}$ are second-order, the diagonal terms given by Eq. (13) are first order, due to the constraint on the columns of the cross-orthogonality matrix. Substituting Eq. (13) into Eq. (16) indicates that $\boldsymbol{\delta}_M$ has zeros on its diagonal. The first-order representation of the constrained substructure modal mass uncertainty is then given by

$$\Delta\mathbf{m}_{jj} = \Delta_{Mjj} \tag{18}$$

$$\Delta\mathbf{m}_{ij} = -\Delta\gamma_{ij} - \Delta\gamma_{ji}, \quad i \neq j \tag{19}$$

Using the same approach for the truth stiffness and mode shapes produces

$$\boldsymbol{\phi}_T^{\mathrm{T}}\mathbf{K}_{\mathrm{Too}}\boldsymbol{\phi}_T = \boldsymbol{\Omega}+\boldsymbol{\delta}_K+\Delta\mathbf{k}+\Delta\boldsymbol{\gamma}^{\mathrm{T}}\Delta\mathbf{k}+\Delta\mathbf{k}\Delta\boldsymbol{\gamma}+\Delta\boldsymbol{\gamma}^{\mathrm{T}}\Delta\mathbf{k}\Delta\boldsymbol{\gamma} \tag{20}$$

in which

$$\boldsymbol{\delta}_K = \boldsymbol{\Omega}\Delta\boldsymbol{\gamma}+\Delta\boldsymbol{\gamma}^{\mathrm{T}}\boldsymbol{\Omega}+\Delta\boldsymbol{\gamma}^{\mathrm{T}}\boldsymbol{\Omega}\Delta\boldsymbol{\gamma} \tag{21}$$

The left side of Eq. (20) can also be expressed in the form $\boldsymbol{\phi}_T^{\mathrm{T}}\mathbf{K}_{Too}\boldsymbol{\phi}_T = \boldsymbol{\Omega}_T+\boldsymbol{\Delta}_K$, where Δ_K is a diagonal matrix representing the uncertainty in the generalized stiffnesses in the truth modal space. Eliminating second-order terms in Eq. (20) yields

$$\Delta\mathbf{k} = \Delta\boldsymbol{\Omega}+\Delta_K-\boldsymbol{\delta}_K = 2\boldsymbol{\omega}\Delta\boldsymbol{\omega}+\Delta_K-\boldsymbol{\delta}_K \tag{22}$$

where $\Delta\boldsymbol{\omega}$ is the uncertainty in the fixed substructure frequencies. As in the mass uncertainty analysis, the off-diagonal terms of matrix $\Delta\boldsymbol{\gamma}^{\mathrm{T}}\boldsymbol{\Omega}\Delta\boldsymbol{\gamma}$ in $\boldsymbol{\delta}_K$ are second order and can be ignored. Applying the constraint in Eq. (14), the diagonal terms of $\boldsymbol{\delta}_K$ are given by

$$\delta_{Kjj} = 2\boldsymbol{\Omega}_j\Delta\gamma_{jj}+\sum_{i=1}^{n_q}\Delta\gamma_{ij}^2\boldsymbol{\Omega}_i = \sum_{\substack{i=1\\ i\neq j}}^{n_q}\Delta\gamma_{ij}^2(\boldsymbol{\Omega}_i-\boldsymbol{\Omega}_j) \tag{23}$$

which are also second order. In addition, it can be easily shown that to first order $\Delta_K=\Delta_M\boldsymbol{\Omega}$. The first-order representation of the modal stiffness uncertainty is then given by

$$\Delta k_{jj} = 2\omega_j\Delta\omega_j+\Delta_{Mjj}\boldsymbol{\Omega}_j \tag{24}$$

$$\Delta k_{ij} = -\Delta\gamma_{ij}\boldsymbol{\Omega}_i-\Delta\gamma_{ji}\boldsymbol{\Omega}_j, \quad i\neq j \tag{25}$$

The perturbation results presented here differ from those presented by Hasselman [20] in the expressions for the diagonal terms Δm_{jj} and Δk_{jj} in Eqs. (18) and (24). As mentioned previously, this is due to the fact that in this work the truth modes are assumed to be normalized with respect to the nominal FEM mass matrix. In Hasselman's formulation

$$\Delta m_{jj} = -2\Delta\gamma'_{jj} = \Delta_{Mjj} \tag{26}$$

in which $\Delta\boldsymbol{\gamma}'$ is the cross-orthogonality matrix where the truth modes are normalized with respect to the truth mass matrix. The uncertainty formulation presented here is consistent with the definition of cross-orthogonality that is accepted and employed in practice [2]. In this case, uncertainty in generalized mass Δ_{Mjj} is independent of uncertainty in the cross-generalized mass $\Delta\gamma_{jj}$. This makes sense because as each set of truth modes is normalized to the nominal mass matrix, the information regarding its normalized length in truth modal space is lost.

2.2. Uncertainty in unconstrained substructure

In this subsection, the uncertainty in the fixed interface modal mass and stiffness matrices is related to uncertainty in the unconstrained substructure modal matrices using the CB representation. Only uncertainty in the interior of the substructure is considered. Future research will consider the more difficult, but very important, problem of uncertainty at the interface.

When attempting to decouple the effects of uncertainty in the interior of a substructure (o-set) from uncertainty in its interface (a-set), it is important to realize that in general, the corresponding submatrices of $\Delta\mathbf{K}$ and $\Delta\mathbf{M}$ are not independent. This is due to the fact that the perturbed, or truth, mass and stiffness matrices must maintain their appropriate sign-definiteness characteristics, such that they correspond to an actual possible structure. In the case of mass, the o-set and a-set can, in general, be considered as decoupled. Therefore, $\Delta\mathbf{M}_{oa} = \Delta\mathbf{M}_{ao}^{\mathrm{T}}$ can be assumed to be null, and $\Delta\mathbf{M}_{\mathrm{oo}}$ can be varied independently of $\Delta\mathbf{M}_{aa}$, while still maintaining the symmetry and positive definiteness of the truth physical mass matrix $\mathbf{M}_{\mathrm{T}}=\mathbf{M}+\Delta\mathbf{M}$. Using Eq. (3), uncertainty in the CB mass representation can be expressed relative to the nominal CB vector space as

$$\Delta\mathbf{M}_{\mathrm{CB}} = \mathbf{T}^{\mathrm{T}}\Delta\mathbf{M}\mathbf{T} = \begin{bmatrix}\Delta\mathbf{m} & \Delta\mathbf{M}_{qa}\\ \Delta\mathbf{M}_{aq} & \Delta\mathbf{M}_S\end{bmatrix} \tag{27}$$

Uncertainty in the mass coupling between fixed interface modes and interface degrees of freedom in Eq. (27) is given by $\Delta\mathbf{M}_{qa}$ and its transpose. If all the fixed interface modes are retained, then they span the vectors in the constraint mode partition $\boldsymbol{\psi}$. In this work, it will be assumed that enough fixed modes are retained such that $\boldsymbol{\psi}\approx\boldsymbol{\phi}\boldsymbol{\eta}$ where $\boldsymbol{\eta}$ is a $n_q\times n_a$ matrix that can be computed using $\boldsymbol{\eta}=\boldsymbol{\phi}^{\mathrm{T}}M_{oo}\boldsymbol{\psi}$, and n_a is the number of interface degrees of freedom. The uncertainty in the mass coupling term is then given by

$$\begin{aligned}\Delta\mathbf{M}_{qa} = \boldsymbol{\phi}^T\Delta\mathbf{M}_{oo}\boldsymbol{\psi} = \boldsymbol{\phi}^{\mathrm{T}}\Delta\mathbf{M}_{oo}\boldsymbol{\phi}\boldsymbol{\eta} = \Delta\mathbf{m}\boldsymbol{\eta}\\ \Delta\mathbf{M}_{aq} = \boldsymbol{\eta}^{\mathrm{T}}\Delta\mathbf{m}\end{aligned} \tag{28}$$

Likewise, the uncertainty in the statically reduced mass $\mathbf{M}_S$ can be expressed as

$$\Delta\mathbf{M}_S = \boldsymbol{\psi}^{\mathrm{T}}\Delta\mathbf{M}_{oo}\boldsymbol{\psi} = \eta^{\mathrm{T}}\phi^{\mathrm{T}}\Delta\mathbf{M}_{oo}\phi\boldsymbol{\eta} = \boldsymbol{\eta}^{\mathrm{T}}\Delta\mathbf{m}\boldsymbol{\eta} \tag{29}$$

In the case of stiffness, the o-set and a-set are not decoupled, and the corresponding uncertainty submatrices $\Delta\mathbf{K}_{oo}$, $\Delta\mathbf{K}_{oa}$, and $\Delta\mathbf{K}_{aa}$ cannot vary independently. For example, assuming that there is no uncertainty in the substructure rigid body modes, independent of the truth physical stiffness $\mathbf{K}_T=\mathbf{K}+\Delta\mathbf{K}$, the rigid body modes must always lie in its null space. This then implies that the rigid body modes must also lie in the null space of the stiffness uncertainty $\Delta\mathbf{K}$, which produces a constraint between its submatrices. In an analogous manner, the interior stiffness uncertainty can be decoupled from the interface uncertainty by assuming there is no uncertainty in the constraint modes $\boldsymbol{\Psi}$, resulting in $\Delta\mathbf{K}\boldsymbol{\Psi}=0$. Expanding this result produces

$$\begin{aligned}\Delta\mathbf{K}_{oa}=\Delta\mathbf{K}_{ao}^{\mathrm{T}}&=-\Delta\mathbf{K}_{oo}\boldsymbol{\psi}\\ \Delta\mathbf{K}_{aa}&=\boldsymbol{\psi}^{T}\Delta K_{oo}\boldsymbol{\psi}\end{aligned}\tag{30}$$

Therefore, if the interior uncertainty $\Delta\mathbf{K}_{oo}$ is specified, the uncertainty in the interface stiffness partitions is dictated. The uncertainty in the CB stiffness representation is then given by

$$\Delta\mathbf{K}_{CB}=\mathbf{T}^{\mathrm{T}}\Delta\mathbf{K}\mathbf{T}=\begin{bmatrix}\Delta\mathbf{k} & 0\\ 0 & 0\end{bmatrix}\tag{31}$$

For n_m unconstrained substructure normal modes in CB coordinates $\boldsymbol{\Phi}_{\mathrm{CB}}=\begin{bmatrix}\boldsymbol{\Phi}_q^{\mathrm{T}} & \boldsymbol{\Phi}_a^{\mathrm{T}}\end{bmatrix}^{\mathrm{T}}$, the uncertainty in modal mass and stiffness can then be computed using

$$\Delta\mathcal{M}=\boldsymbol{\Phi}_{\mathrm{CB}}^{\mathrm{T}}\Delta M_{\mathrm{CB}}\boldsymbol{\Phi}_{\mathrm{CB}},\quad \Delta\mathcal{K}=\boldsymbol{\Phi}_{\mathrm{CB}}^{\mathrm{T}}\Delta K_{\mathrm{CB}}\boldsymbol{\Phi}_{\mathrm{CB}}\tag{32}$$

or after expansion

$$\Delta\mathcal{M}=\boldsymbol{\Phi}_q^{\mathrm{T}}\Delta\mathbf{m}\boldsymbol{\Phi}_q+\boldsymbol{\Phi}_q^{\mathrm{T}}\Delta\mathbf{m}\boldsymbol{\eta}\boldsymbol{\Phi}_a+\boldsymbol{\Phi}_a^{\mathrm{T}}\boldsymbol{\eta}^{\mathrm{T}}\Delta\mathbf{m}\boldsymbol{\Phi}_q+\boldsymbol{\Phi}_a^{\mathrm{T}}\boldsymbol{\eta}^{\mathrm{T}}\Delta\mathbf{m}\boldsymbol{\eta}\boldsymbol{\Phi}_a\tag{33}$$

$$\Delta\mathcal{K}=\boldsymbol{\Phi}_q^{\mathrm{T}}\Delta\mathbf{k}\boldsymbol{\Phi}_q\tag{34}$$

Eqs. (33) and (34) relate the uncertainty in fixed interface modal mass and stiffness to free interface modal mass and stiffness.

2.3. Uncertainty propagation

Linear covariance propagation [12] will be used to propagate uncertainty from the fixed substructure into the unconstrained substructure. In order to do so, the uncertainty matrices in Eqs. (33) and (34) must be transformed to vectors using the vec($\mathbf{X}$) operator [22] where the terms in matrix $\mathbf{X}$ are stacked column-wise into a single vector. It can be shown that for compatible matrices $\mathbf{A}$, $\mathbf{X}$, and $\mathbf{B}$

$$\mathrm{vec}(\mathbf{AXB})=(\mathbf{B}^{\mathrm{T}}\otimes\mathbf{A})\mathrm{vec}(\mathbf{X})\tag{35}$$

in which the symbol $\otimes$ represents the Kronecker product between two matrices [22], given by

$$\mathbf{A}\otimes\mathbf{B}=\begin{bmatrix}A_{11}\mathbf{B} & A_{11}\mathbf{B} & \cdots & A_{1m}\mathbf{B}\\ A_{21}\mathbf{B} & A_{22}\mathbf{B} & \cdots & \vdots\\ \vdots & \vdots & \ddots & \vdots\\ A_{n1}\mathbf{B} & \cdots & \cdots & A_{nm}\mathbf{B}\end{bmatrix}\tag{36}$$

where $\mathbf{A}$ is an $n\times m$ matrix.

Using these results, the expression for mass uncertainty in Eq. (33) can be rewritten as

$$\mathrm{vec}(\Delta\mathcal{M})=\left[\left(\boldsymbol{\Phi}_q^{\mathrm{T}}\otimes\boldsymbol{\Phi}_q^{\mathrm{T}}\right)+\left(\boldsymbol{\Phi}_q^{\mathrm{T}}\otimes\boldsymbol{\Phi}_a^{\mathrm{T}}\boldsymbol{\eta}^{\mathrm{T}}\right)+\left(\boldsymbol{\Phi}_a^{\mathrm{T}}\boldsymbol{\eta}^{\mathrm{T}}\otimes\boldsymbol{\Phi}_q^{\mathrm{T}}\right)+\left(\boldsymbol{\Phi}_a^{\mathrm{T}}\boldsymbol{\eta}^{\mathrm{T}}\otimes\boldsymbol{\Phi}_a^{\mathrm{T}}\boldsymbol{\eta}^{\mathrm{T}}\right)\right]\mathrm{vec}(\Delta\mathbf{m})$$

or

$$\mathrm{vec}(\Delta\mathcal{M})=\tilde{\mathbf{Q}}\,\mathrm{vec}(\Delta\mathbf{m})\tag{37}$$

in which vec($\Delta\mathcal{M}$) is a $n_m^2\times 1$ vector, vec($\Delta\mathbf{m}$)is $n_q^2\times 1$, and each of the matrices in the brackets is $n_m^2\times n_q^2$. The uncertainty matrices $\Delta\mathbf{m}$ and $\Delta\mathcal{M}$ are both symmetric, so only the lower triangular terms are included in the propagation analysis. The vech($\mathbf{X}$) operator [22] can be used to extract the lower triangular terms of a symmetric $n\times n$ matrix and stack them column-wise in a $n(n+1)/2$ dimensional column vector. The elimination matrix, $\mathbf{S}_n$ [23], can be used to relate the vec($\mathbf{X}$) and vech($\mathbf{X}$) operators as

$$\mathrm{vech}(\mathbf{X})=\mathbf{S}_n\mathrm{vec}(\mathbf{X})\tag{38}$$

where $\mathbf{S}_n$ is a $[n(n+1)/2]\times n^2$ full row rank matrix with a single 1.0 in each row. The inverse elimination, or duplication, matrix can be formed such that

$$\mathrm{vec}(\mathbf{X})=\mathbf{S}_n^{-1}\mathrm{vech}(\mathbf{X})\tag{39}$$

in which $\mathbf{S}_n^{-1}$ is an $n^2 \times [n(n+1)/2]$ full column rank matrix, also with a single 1.0 in each row, and $\mathbf{S}_n\mathbf{S}_n^{-1} = \mathbf{I}_{n(n+1)/2}$. Applying these definitions to Eq. (37) produces

$$\text{vech}(\Delta\mathcal{M}) = \mathbf{S}_{n_m}\tilde{\mathbf{Q}}\mathbf{S}_{n_q}^{-1}\text{vech}(\Delta\mathbf{m}) \tag{40}$$

or using the simplifying notation, $\Delta p_{\mathcal{M}} = \text{vech}(\Delta\mathcal{M})$, $\Delta\mathbf{p}_m = \text{vech}(\Delta\mathbf{m})$, and $\tilde{\mathbf{T}} = \mathbf{S}_{n_m}\tilde{\mathbf{Q}}\mathbf{S}_{n_q}^{-1}$

$$\Delta\mathbf{p}_{\mathcal{M}} = \tilde{\mathbf{T}}\Delta\mathbf{p}_m \tag{41}$$

where $\tilde{\mathbf{T}}$ is of dimension $[n_m(n_m+1)/2] \times [n_q(n_q+1)/2]$. A parallel analysis for stiffness produces

$$\Delta\mathbf{p}_{\mathcal{K}} = \tilde{\mathbf{T}}_{qq}\Delta\mathbf{p}_k \tag{42}$$

where $\tilde{\mathbf{T}}_{qq} = \mathbf{S}_{n_m}\left(\Phi_q^{\mathrm{T}} \otimes \Phi_q^{\mathrm{T}}\right)\mathbf{S}_{n_q}^{-1}$.

Uncertainty in modal mass at the fixed interface substructure level can be related to uncertainty in the unconstrained substructure modal mass using linear covariance propagation [12]. Taking the expectation, $E()$, of the outer product of Eq. (41) with itself gives

$$E(\Delta\mathbf{p}_{\mathcal{M}}\Delta\mathbf{p}_{\mathcal{M}}^{\mathrm{T}}) = \mathbf{C}_{\Delta\mathcal{M}} = \tilde{\mathbf{T}}E(\Delta\mathbf{p}_m\Delta\mathbf{p}_m^{\mathrm{T}})\tilde{\mathbf{T}}^{\mathrm{T}} = \tilde{\mathbf{T}}\mathbf{C}_{\Delta m}\tilde{\mathbf{T}}^{\mathrm{T}} \tag{43}$$

in which $\mathbf{C}_{\Delta\mathbf{M}}$ and $\mathbf{C}_{\Delta\mathrm{m}}$ are the covariance matrices for uncertainty in modal mass at the free- and fixed interface levels, respectively. The analogous modal stiffness equation is given by

$$\mathbf{C}_{\Delta\mathcal{K}} = \tilde{\mathbf{T}}_{qq}\mathbf{C}_{\Delta k}\tilde{\mathbf{T}}_{qq}^{\mathrm{T}} \tag{44}$$

The covariance matrices for modal mass and stiffness can be set at the fixed interface level by specifying truth-analysis correlation uncertainty, and Eqs. (43) and (44) can be employed to compute the corresponding covariance matrices at the free substructure level. The diagonal terms in the covariance matrices correspond to the mean square values, or variances, of the mass and stiffness uncertainties in $\Delta\mathbf{p}_X$. This information can then be used to determine the statistics of the correlation metrics at the unconstrained substructure level. This will be illustrated in the next subsection and through a numerical example.

In practice, substructures are usually tested in a free–free configuration due to difficulties in constructing sufficiently rigid test fixtures. Therefore, it is important to be able to specify test- or truth-analysis correlation uncertainty at the free substructure stage, and then propagate it back into modal mass and stiffness uncertainty at the fixed level, which can then be propagated into system level correlation uncertainty. The inverse covariance propagation relations are given by

$$\mathbf{C}_{\Delta m} = \tilde{\mathbf{T}}^{\dagger}\mathbf{C}_{\Delta\mathcal{M}}\tilde{\mathbf{T}}^{\dagger\mathrm{T}} \quad \text{and} \quad \mathbf{C}_{\Delta k} = \tilde{\mathbf{T}}_{qq}^{\dagger}\mathbf{C}_{\Delta\mathcal{K}}\tilde{\mathbf{T}}_{qq}^{\dagger\mathrm{T}} \tag{45}$$

in which $\tilde{\mathbf{T}}^{\dagger}$ represents the generalized inverse of the rectangular matrix $\tilde{\mathbf{T}} = \mathbf{U}_{\tilde{T}}\mathbf{S}_{\tilde{T}}\mathbf{V}_{\tilde{T}}^{\mathrm{T}}$ given by

$$\tilde{\mathbf{T}}^{\dagger} = \mathbf{V}_{\tilde{T}}\mathbf{S}_{\tilde{T}}^{-1}\mathbf{U}_{\tilde{T}}^{\mathrm{T}} \tag{46}$$

where singular value decomposition of $\tilde{\mathbf{T}}$ has been used, and diagonal matrix $\mathbf{S}_{\tilde{T}}$ has been truncated to the non-zero singular values, as well as the corresponding orthonormal principal vectors $\mathbf{U}_{\tilde{T}}$ and $\mathbf{V}_{\tilde{T}}$. Generalized inverse $\tilde{\mathbf{T}}_{qq}^{\dagger}$ is computed in a similar manner.

2.4. Specification of covariance matrices

In the preceding work by Hasselman [20] on the propagation of test-analysis correlation uncertainty, the covariance matrices for modal mass and stiffness uncertainty were derived using databases containing the results of previous test-analysis correlations of similar spacecraft. One of the main contributions of this work is the derivation of the form of the covariance matrices in terms of test- or truth-analysis correlation uncertainty using analytical and numerical experimentation results. A user can then specify correlation uncertainty and perform numerical experiments to study its effects on substructure, or ultimately system correlation.

It is assumed that the expected values of the uncertainty in the physical mass and stiffness matrices, $E(\Delta\mathbf{M})$ and $E(\Delta\mathbf{K})$, are both zero. Therefore, the same is true for the modal matrices, $E(\Delta\mathbf{m})=0$ and $E(\Delta\mathbf{k})=0$. This then implies that the expected value of the uncertainty in the generalized masses, $E(\Delta_{Mjj})=0$, and the expected value of uncertainties in natural frequencies, $E(\Delta\omega_j)=0$. Eqs. (19) and (25) can be combined to give

$$\Delta\gamma_{ij} = \frac{1}{(\boldsymbol{\Omega}_i - \boldsymbol{\Omega}_j)}\left[\boldsymbol{\Omega}_j\Delta m_{ij} - \Delta k_{ij}\right], \quad i \neq j \tag{47}$$

which implies that the expected values of the off-diagonal terms in the cross-orthogonality uncertainty are also zero, $E(\Delta\gamma_{ij})=0$. In contrast with Hasselman's work [20], due to the normalization of the truth modes with respect to the nominal FEM mass, the expected values of the diagonal terms in the cross-orthogonality uncertainty matrix are not zero, $E(\Delta\gamma_{jj}) \neq 0$, meaning that $E(\gamma_{jj}) \neq 1$.

As mentioned, besides the derivation of analytical expressions, numerical experiments were relied upon to determine some of the required terms within the modal covariance matrices. A single numerical experiment consisted of Monte

Carlo analysis, where at each iteration, the nominal FEM fixed interface mass and stiffness matrices were randomized using the Maximum Entropy approach developed by Soize [24]. A dispersion level is selected that can be thought of as being analogous to the global fractional uncertainty believed to exist in the matrix, and then the matrix is randomized subject to the constraints of maintaining symmetry and positive definiteness. Details of the process can be found in Soize's paper [24]. The advantage of this nonparametric approach, over the usual parameter sensitivity or perturbation methods, is that this randomization process automatically accounts for uncertainties that are not easily described by model parameters, such as model form, geometry, joints, etc. A specific application will be discussed in Section 3.

Through extensive numerical experimentation, it was found that the covariance matrices for both the modal mass and stiffness are diagonal, meaning that the terms within each of the vectors $\Delta\mathbf{p}_m$ and $\Delta\mathbf{p}_k$ are uncorrelated. It was also found that off-diagonal cross-orthogonality uncertainty term $\Delta\gamma_{ij}$ is strongly correlated with the term $\Delta\gamma_{ji}$ across the diagonal, but is not correlated with any of the other off-diagonal terms. Eqs. (19) and (25) can be combined to produce the expression

$$\Delta m_{ij}\Delta k_{ij} = \boldsymbol{\Omega}_i\Delta\gamma_{ij}^2 + \boldsymbol{\Omega}_j\Delta\gamma_{ji}^2 + (\boldsymbol{\Omega}_i+\boldsymbol{\Omega}_j)\Delta\boldsymbol{\gamma}_{ij}\Delta\boldsymbol{\gamma}_{ji} \tag{48}$$

For the assumed stochastic model, numerical experiments also showed that Δm_{ij} and Δk_{ij} are not correlated, $E(\Delta m_{ij}\Delta k_{ij})=0$. Eq. (48) then gives

$$E(\Delta\boldsymbol{\gamma}_{ij}\Delta\boldsymbol{\gamma}_{ji}) = \frac{-1}{(\boldsymbol{\Omega}_i+\boldsymbol{\Omega}_j)}\left[\boldsymbol{\Omega}_i E\left(\Delta\gamma_{ij}^2\right)+\boldsymbol{\Omega}_j E\left(\Delta\gamma_{ji}^2\right)\right] \tag{49}$$

Using Eq. (47), the expression in Eq. (49) can also be written in the form

$$E(\Delta\boldsymbol{\gamma}_{ij}\Delta\boldsymbol{\gamma}_{ji}) = \frac{-1}{(\boldsymbol{\Omega}_i-\boldsymbol{\Omega}_j)^2}\left[E\left(\Delta k_{ij}^2\right)+\boldsymbol{\Omega}_i\boldsymbol{\Omega}_j E\left(\Delta m_{ij}^2\right)\right] \tag{50}$$

An inspection of Eq. (50) indicates that $E(\Delta\gamma_{ij}\Delta\gamma_{ji})\le 0$, and as Ω_i approaches Ω_j, the correlation between $\Delta\gamma_{ij}$ and $\Delta\gamma_{ji}$ increases. The variance of terms Δm_{ij} can be computed based on Eqs. (19) and (49), yielding the expression

$$E(\Delta m_{ij}^2) = \frac{\boldsymbol{\Omega}_j-\boldsymbol{\Omega}_i}{\boldsymbol{\Omega}_j+\boldsymbol{\Omega}_i}\left[E(\Delta\boldsymbol{\gamma}_{ij}^2)-E(\Delta\boldsymbol{\gamma}_{ji}^2)\right] \tag{51}$$

Turning to modal stiffness uncertainty terms, Eq. (24) can be squared to yield

$$\Delta k_{jj}^2 = 4\boldsymbol{\Omega}_j\Delta\boldsymbol{\omega}_j^2 + 4\boldsymbol{\Omega}_j^{3/2}\Delta\boldsymbol{\omega}_j\Delta_{Mjj} + \boldsymbol{\Omega}_j^2\Delta_{Mjj}^2 \tag{52}$$

Assuming that mass and stiffness uncertainties are not correlated, $E(\Delta m_{jj}\Delta k_{\mathrm{jj}})=0$, then Eq. (24) can be used to show that $E(\Delta\boldsymbol{\Omega}_j\Delta m_{jj}) = -\boldsymbol{\Omega}_j^2 E(\Delta_{Mjj}^2)$. Eq. (51) then produces the variance of Δk_{ii} as

$$E(\Delta k_{jj}^2) = 4\boldsymbol{\Omega}_j E(\Delta\boldsymbol{\omega}_j^2) - \boldsymbol{\Omega}_j^2 E(\Delta_{Mjj}^2) \tag{53}$$

The variance of off-diagonal terms Δk_{ij} can be computed based on Eqs. (25) and (49), giving

$$E(\Delta k_{ij}^2) = \frac{\boldsymbol{\Omega}_j-\boldsymbol{\Omega}_i}{\boldsymbol{\Omega}_j+\boldsymbol{\Omega}_i}\left[\boldsymbol{\Omega}_j^2 E(\Delta\boldsymbol{\gamma}_{ji}^2)-\boldsymbol{\Omega}_i^2 E(\Delta\boldsymbol{\gamma}_{ij}^2)\right] \tag{54}$$

With the previous expressions available, the analyst can compute covariance matrices for modal mass and stiffness by specifying the variances of the natural frequencies, $E(\Delta\boldsymbol{\omega}_j^2)$, the variances of the generalized masses, $E(\Delta_{Mjj}^2)$, and the variances of the off-diagonal terms in each column of the cross-orthogonality matrix, $E(\Delta\gamma_{ij}^2)$. According to Eq. (14), the mean-square values of the cross-generalized masses, $E(\gamma_{jj}^2)$ can also be computed using

$$E(\boldsymbol{\gamma}_{jj}^2) = 1 - \sum_{\substack{i=1\\ i\neq j}}^{n_q} E(\Delta\boldsymbol{\gamma}_{ij}^2) \tag{55}$$

Variances of the off-diagonal terms $\Delta\gamma_{ij}$ may be specified individually, or in any manner the analyst desires, subject to the constraints that $E(\gamma_{jj}^2)\le 1$ and

$$1 \le \frac{E(\Delta\boldsymbol{\gamma}_{ji}^2)}{E(\Delta\boldsymbol{\gamma}_{ij}^2)} \le \frac{\boldsymbol{\Omega}_i^2}{\boldsymbol{\Omega}_j^2} \tag{56}$$

which is derived from Eqs. (51) and (54). Note also that based on Eq. (53), $E(\Delta\boldsymbol{\omega}_j^2)$ and $E(\Delta_{Mjj}^2)$ must satisfy the inequality $4E(\Delta\boldsymbol{\omega}_j^2)\ge\boldsymbol{\Omega}_j E(\Delta_{Mjj}^2)$. Using the results presented in this section, the covariance matrices for uncertainty in modal mass and stiffness can then be easily generated, whether they are related to a free- or fixed interface substructure.

After the assumed uncertainty in the truth-analysis correlation metrics is propagated in either the forward or reverse directions into uncertainty in free- or fixed interface substructure modal mass and stiffness, uncertainty in the corresponding correlation metrics must then be recovered. Squaring Eq. (47) and applying the expectation operator produces the variance of the off-diagonal cross-orthogonality terms

$$E(\Delta\boldsymbol{\gamma}_{ij}^2) = \frac{1}{(\boldsymbol{\Omega}_i-\boldsymbol{\Omega}_j)^2}\left[E(\Delta k_{ij}^2)+\boldsymbol{\Omega}_j^2 E(\Delta m_{ij}^2)\right] \tag{57}$$

Eq. (53) gives the variance of the natural frequencies as

$$E(\Delta\omega_j^2) = \frac{1}{4\Omega_j}\left[E(\Delta k_{jj}^2) + \Omega_j^2 E(\Delta m_{jj}^2)\right] \tag{58}$$

Numerical experiments also showed that the off-diagonal uncertainty terms $\Delta\gamma_{ij}$ are not only zero mean, but normally distributed, and within each column, independent. Assuming, for example, a forward propagation from fixed into free substructure modes, Eq. (14) indicates that the term $c_j = 1-\gamma_{jj}^2$ is the sum of the squares of n_m-1 zero mean, normally distributed variables $\Delta\gamma_{ij}$. If the terms $\Delta\gamma_{ij}$ all had unit variance, c_j would be represented by a chi-square distribution with n_m-1 degrees of freedom [3]. In this case, however, the off-diagonal terms $\Delta\gamma_{ij}$ will have different non-unit variances. Therefore, c_j follows a generalized chi-square distribution. In general, the number of degrees of freedom is not equal to n_m-1 because many of the nominal FEM modes do not couple strongly with the jth truth mode, meaning many of the terms $\Delta\gamma_{ij}$ are small. As the number of terms that significantly contribute increases, the probability distribution approaches a normal distribution.

In terms of standard normal variables z_i, c_j can be written as

$$c_j = 1-\gamma_{jj}^2 = \sum_{\substack{i=1\\ i\neq j}}^{n_m} \sigma_i^2 z_i^2 \tag{59}$$

where $\sigma_i^2 = E(\Delta\gamma_{ij}^2)$ are the off-diagonal cross-orthogonality variances recovered for the jth column using Eq. (57). A distribution for c_j can then be constructed by taking a linear combination of single degree of freedom chi-square distributions $\chi^2(1)$ using

$$c_j = \sum_{\substack{i=1\\ i\neq j}}^{n_m} \sigma_i^2 \chi^2(1) \tag{60}$$

The $(1-\alpha)$th percentile for c_j can easily be computed and then the corresponding value for the jth cross-generalized mass, given by $\gamma_{jj\alpha} = \sqrt{1-c_{j\alpha}}$, can be compared to designated correlation metric criteria.

3. Numerical example

The numerical example considered in this paper is a simple representation of a communications satellite, called Qsat, shown in Fig. 1. The substructure that will be considered for uncertainty propagation consists of the Earth pointing (+Z) reflector and tower that is mounted to the top of the bus via bars as shown in the figure. The reflector-tower substructure has 18 interface degrees of freedom (3 translations at 6 nodes) and 11,337 interior degrees of freedom. With the interface degrees of freedom constrained, there are 50 substructure modes below 200.0 Hz. In the free–free configuration, there are 56 elastic modes below 200.0 Hz.

Forward propagation from the fixed interface correlation metrics into free interface correlation metrics will be considered first. A numerical experiment was initially performed to investigate the probability distributions of the terms of interest. The Maximum Entropy approach [24] was used to randomize the nominal fixed interface mass and stiffness matrices using a dispersion value of 3.0%. The corresponding modes and frequencies were computed and compared with the nominal modal parameters to yield frequency errors and cross-orthogonalities for 100,000 iterations. As expected, it was found that the uncertainties in the generalized masses, Δ_{Mjj}, frequencies, $\Delta\omega_j$, and off-diagonal cross-orthogonalities, $\Delta\gamma_{ij}$, are all zero mean and normally distributed. Fig. 2 illustrates the estimate of a typical off-diagonal cross-orthogonality probability distribution. Fig. 3 shows the estimated generalized chi-square probability distribution for the term $c_{21} = 1-\gamma_{21,21}^2$, corresponding to free mode 21. The distribution is somewhat skewed to the right because a relatively small number of off-diagonal terms in this column of the cross-orthogonality matrix contribute significantly.

Uncertainty in the 50 fixed interface substructure modes below 200 Hz. was propagated into the first 28 free substructure elastic modes below 150 Hz. A level of uncertainty in the test-analysis correlation metrics for the fixed modes was assumed consistent with Air Force criteria at a 95% confidence level. A two-sigma value of 3.0% was assumed for uncertainty in frequencies $\Delta\omega_j$. A one-sigma value of 0.025 was assumed for uncertainty in the generalized masses, Δ_{Mjj}, which is consistent with the inequality based on Eq. (53) mentioned previously.

For simplicity, uncertainty in off-diagonal cross-orthogonality in each column was limited to two terms directly above and below the diagonal. This implies that each truth mode is coupled with at most four nominal FEM modes that are closest in frequency. This type of behavior is consistent with the constraint in Eq. (56) and typical of test-analysis correlation results [5]. A uniform two-sigma value of 0.10 was then assumed for each $\Delta\gamma_{ij}$. Specifying the number of modes that are coupled within each cross-orthogonality matrix column and the variance of the off-diagonal terms, then constrains the two-sigma value of the cross-generalized mass to be $\gamma_{jj0.05} = \sqrt{(0.1/2)^2\chi_{0.05}^2(4)} = 0.988$. This easily satisfies the Air Force criterion of $\gamma_{jj} \geq 0.95$ for cross-generalized mass. Thirty-three off-diagonal terms $\Delta\gamma_{ij}$ of the assumed critical value would have to be designated in each column to reduce $\gamma_{jj0.05}$ to its critical value of 0.95. This shows that the correlation criterion for the off-diagonal terms, $\Delta\gamma_{ij} \leq 0.05$, is most restrictive.

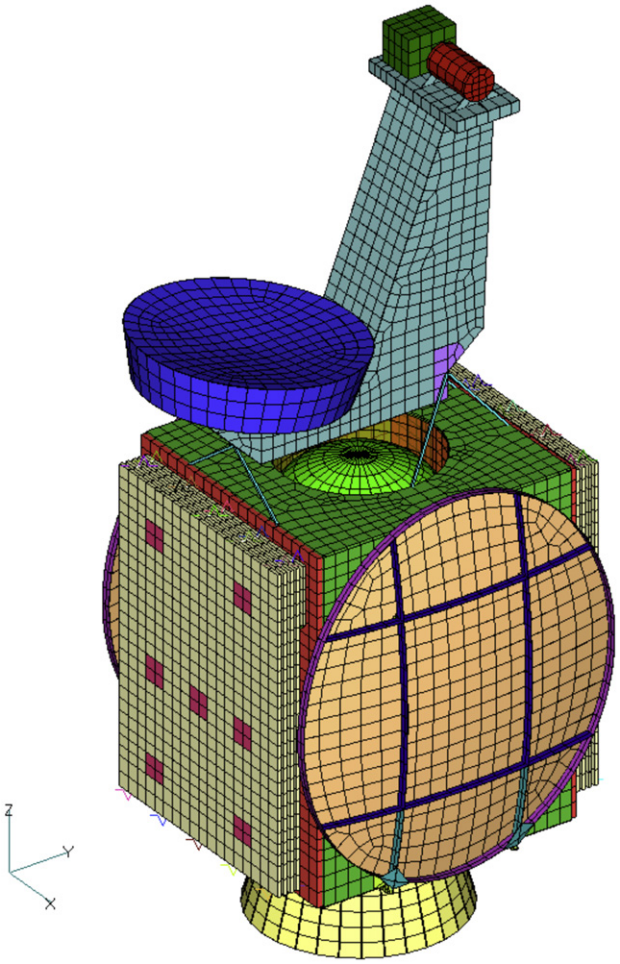

Fig. 1. Finite element model of Qsat communications satellite.

The corresponding modal covariance matrices were then generated using the previously discussed relations and then propagated into free substructure modal matrices using Eqs. (43) and (44). Uncertainty in free substructure frequency was recovered using Eq. (58). The two-sigma frequency uncertainty is shown in Fig. 4. Only mode 10 violates the Air Force frequency correlation criterion at 95% confidence. Uncertainty in cross-orthogonality was recovered using Eq. (57), and then Eq. (55). Root-mean-square cross-orthogonality is shown in Fig. 5. The 95th percentile for cross-generalized mass was determined using Eq. (60). At the 95% confidence level, 14 modes, 1 through 9, 13 through 16, and 26 pass the frequency and the cross-generalized mass correlation criteria. However, only 12 modes, 1 through 9, 13, 16, and 26 satisfy the corresponding off-diagonal cross-orthogonality correlation requirement. This example seems to indicate the possibility that the free substructure modes can be surprisingly sensitive to uncertainty in the fixed substructure modes. In fact, five free modes, 10, 12, and 18 through 20, produce physically unrealizable correlation results due to their hypersensitivity to uncertainty in the fixed substructure modes. Future work will investigate the origin of this sensitivity and its mitigation.

Finally, an application of reverse covariance propagation was investigated for this example. Previous analysis showed that elastic free interface modes 10 through 28 are strongly coupled to fixed interface modes 1 through 25. Therefore, the same level of test-analysis correlation uncertainty assumed in the forward propagation problem was again specified for the 19 free elastic modes and propagated in the reverse direction into the first 25 fixed substructure modes using Eqs. (45) and (46). Root-mean-square uncertainties in fixed substructure modal mass and normalized stiffness are illustrated in Figs. 6 and 7, respectively. Uncertainty levels and coupling in both matrices are consistent with that found in the previous forward propagation problem. In future studies, these fixed substructure modal uncertainty matrices will be propagated into the full system correlation metrics. As expected, the reverse propagation results were also found to be sensitive, depending on the number of singular values retained in the generalized inverse.

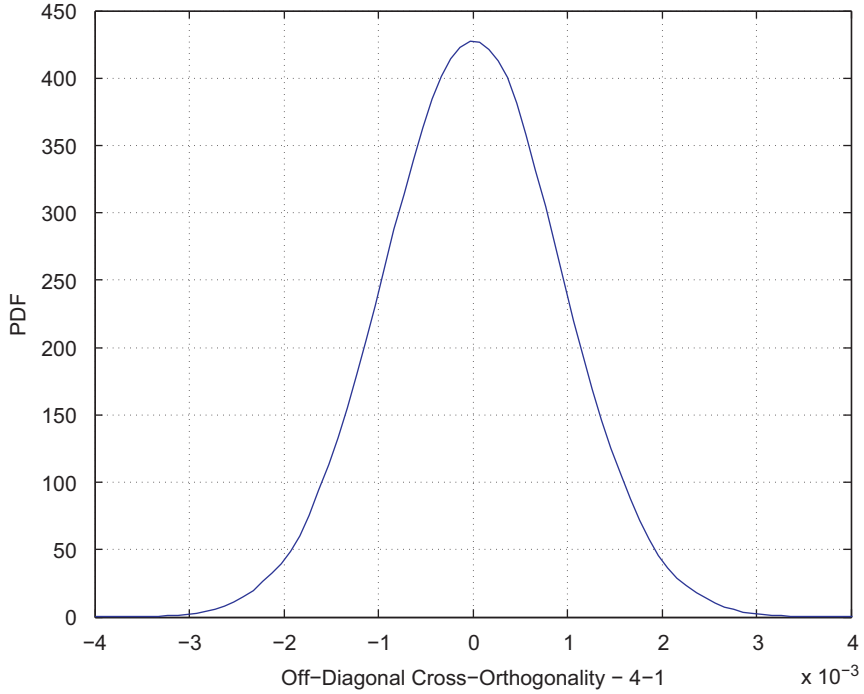

Fig. 2. Estimated PDF for cross-orthogonality term $\Delta\gamma_{5,4}$.

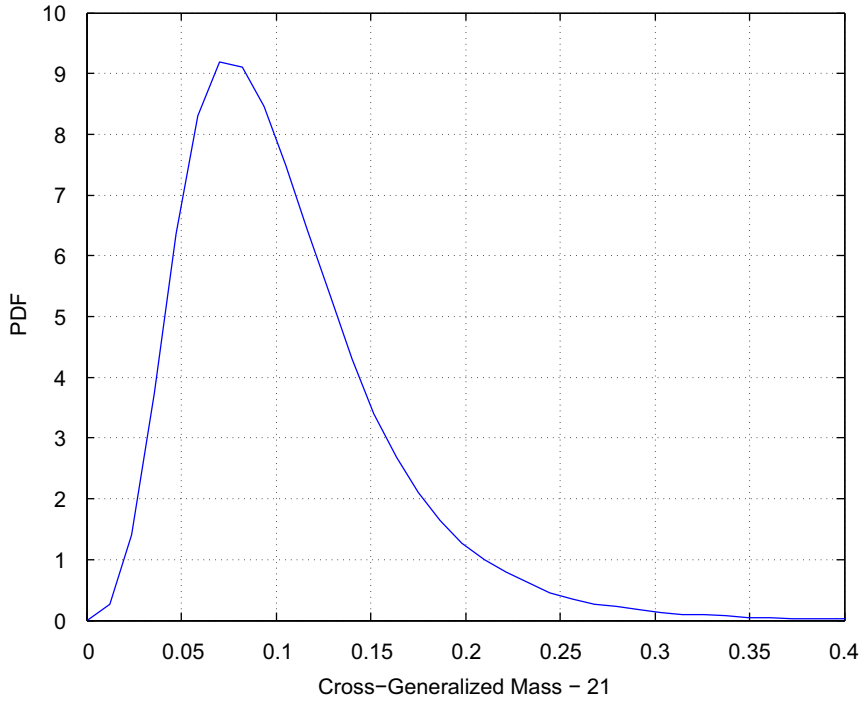

Fig. 3. Estimated PDF for $1-\gamma^2_{21,21}$.

4. Conclusion

A methodology has been presented for studying the effects of uncertainty on metrics used for test-analysis correlation of complex spacecraft that are validated on a substructure-by-substructure basis. The objective is to quantify the level of accuracy required at the substructure level to produce acceptable accuracy at the system level. In preparation for future

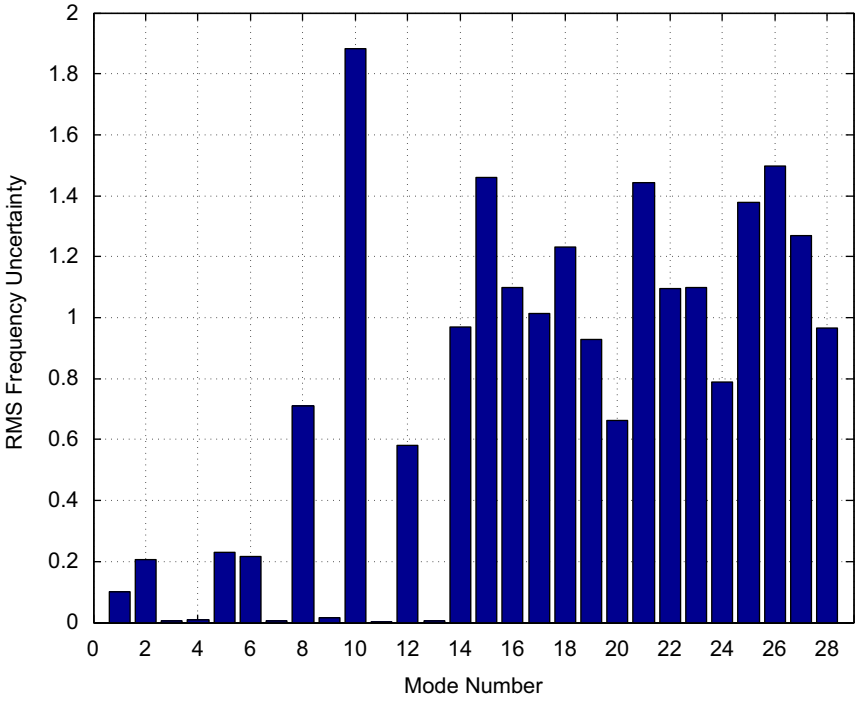

Fig. 4. RMS frequency uncertainty in free substructure modes.

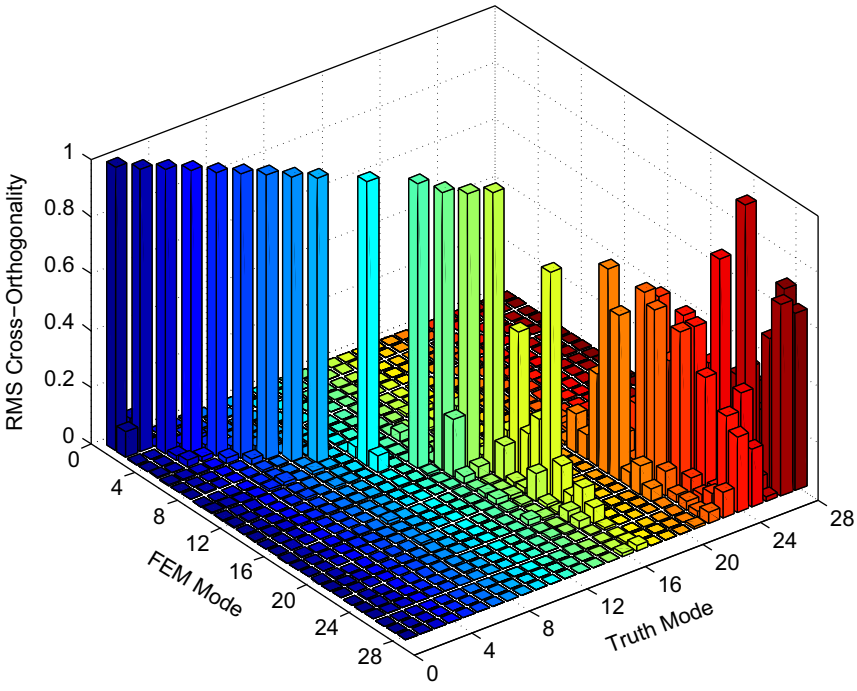

Fig. 5. RMS cross-orthogonality for free substructure.

synthesized system level uncertainty analysis, this paper focused on uncertainty propagation at the substructure level. Linear perturbation analysis was first used to relate uncertainty in accepted test-analysis correlation metrics to substructure modal mass and stiffness uncertainties. A statistical model for the modal based test-analysis correlation metrics was then presented, such that an analyst can specify a corresponding uncertainty covariance matrix. Linear covariance propagation was then used to propagate the specified fixed-interface modal correlation metric uncertainty into

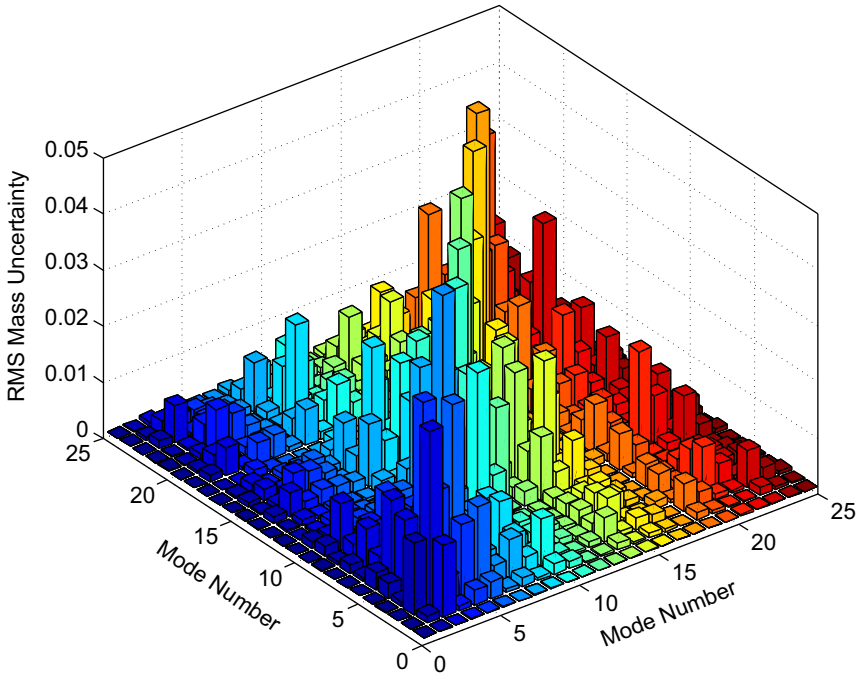

Fig. 6. RMS uncertainty in fixed substructure modal mass.

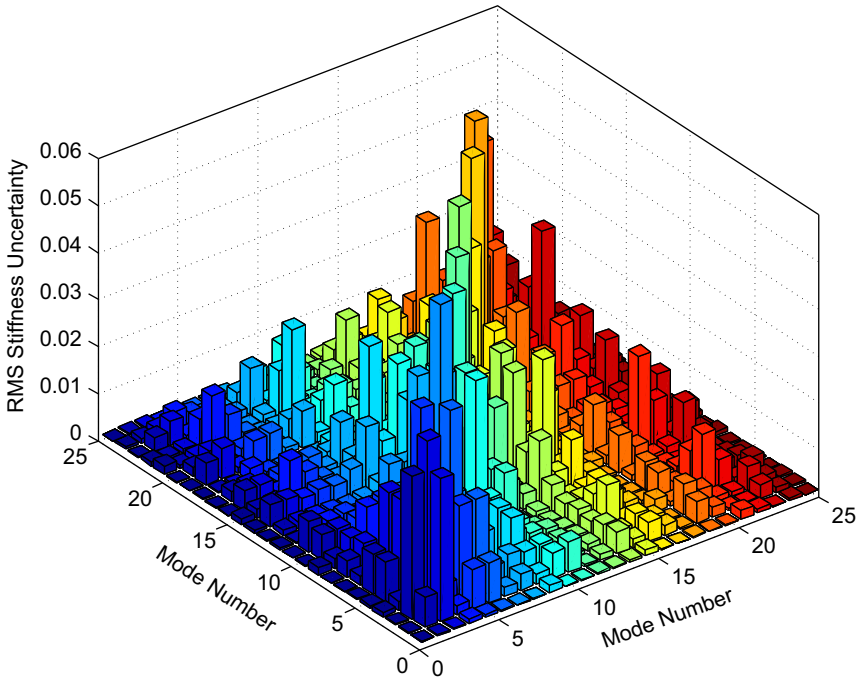

Fig. 7. RMS uncertainty in fixed substructure modal stiffness.

the expected free–free substructure correlation metric uncertainty using a Craig–Bampton substructure representation. Reverse covariance propagation was also investigated, such that assumed uncertainty in free–free substructure correlation metrics can be propagated into the fixed substructure. This propagation direction is of importance because substructure vibration tests are often conducted in a free–free configuration.

The proposed method was applied to a typical substructure from a characteristic spacecraft finite element representation. Frequency and cross-orthogonality uncertainty was assumed in the fixed interface modes at a two-sigma level that just passed the Air Force correlation requirements of 3% frequency accuracy, off-diagonal cross-orthogonality terms less than or equal to 0.10, and cross-generalized mass values greater than or equal to 0.95. This uncertainty was then propagated into the free substructure modal correlation metrics. This particular example showed that some free substructure modes can be very sensitive to uncertainty in the fixed substructure modes. The fixed-interface substructure passed the correlation criteria, but the corresponding free-interface configuration did not pass. The same correlation uncertainty level was then propagated back into the fixed substructure using reverse uncertainty propagation. This also produced some sensitive results. Future work will focus on studying and mitigating the observed sensitivities in the method, as well as determining better ways of specifying meaningful levels of uncertainty in the cross-orthogonality metrics that are the inputs to the approach. The method will then be applied to propagate uncertainty specified at the substructure level into uncertainty at the system level. It is important to remember that the results presented here assume that the mass and stiffness uncertainties are statistically independent.

Organizations, such as NASA and the Air Force make critical decisions on spacecraft performance and survivability based on the results of test-analysis correlation metrics. In order to ensure the success of the new paradigm in finite element model validation where there is no system level test, uncertainty in the substructures must be propagated into the system level correlation metrics. It is believed that the method presented in this paper offers a unique and efficient approach for the required uncertainty propagation. A user can choose to propagate either an assumed level of test-analysis correlation uncertainty, or correlation uncertainty derived from vibration test results. The method is not reliant on the specification of uncertainty in individual model design parameters. It includes all forms of model uncertainty. It is fast, compared with Monte Carlo techniques, and it propagates uncertainty in the correlation metrics directly. Future work will also address the use of Monte Carlo simulation to directly confirm the results of the covariance propagation.

Acknowledgments

This material is based on work supported by the Air Force Office of Scientific Research under grant FA9550-09-1-0180. This funding is gratefully acknowledged. The authors would also like to thank Quartus Engineering, Inc., for the use of the Qsat finite element model example.

References

[1] F.M. Hemez, S.W. Doebling, M.C. Anderson, A brief tutorial on verification and validation, *Proceedings of the 22nd International Modal Analysis Conference*, Dearborn, MI, 2004.
[2] ASME, *Guide for Verification and Validation in Computational Solid Mechanics*, P.T.C.C. 60, Editor, ASME, 2006.
[3] T.L. Paez, Introduction to model validation, *Proceedings of the 27th International Modal Analysis Conference*, Orlando, FL, 2009.
[4] R.L. Mayes, Model correlation and calibration, *Proceedings of the 27th International Modal Analysis Conference*, Orlando, FL, 2009.
[5] T.K. Hasselman, R.N. Coppolino, D.C. Zimmerman, Criteria for modeling accuracy: a state-of-the-practice survey, *Proceedings of the 18th International Modal Analysis Conference*, San Antonio, TX, 2000.
[6] NASA, *NASA-STD-5002, Loads Analyses of Spacecraft and Payloads*, in *NASA-STD-5002*, NASA, 1996.
[7] DoD, *DoD Handbook-340A (USAF), Test Requirements for Launch, Upper Stage, and Space Vehicles, Volume II: Applications and Guidelines*, 1999.
[8] R. Rebba, et al., Statistical validation of simulation models, *International Journal of Materials and Product Technology* 25 (1/2/3) (2006) 164–181.
[9] F.M. Hemez, A.C. Rutherford, R.D. Maupin, Uncertainty analysis of test data shock responses, *Proceedings of the 24th International Modal Analysis Conference*, Saint Louis, MO, 2006.
[10] M. Basseville, A. Benveniste, Handling uncertainties in identification and model validation: a statistical approach, *Proceedings of the 24th International Modal Analysis Conference*, Saint Louis, MO, 2006.
[11] E.J. Bergman, et al. Probalistic investigation of sensitivities of advanced test-analysis model correlation methods, *Proceedings of the 26th International Modal Analysis Conference*, Orlando, FL, 2008.
[12] T.K. Hasselman, J.D. Chrowstowski, Propagation of modeling uncertainty through structural dynamic models, *Proceedings of the 35th Structures, Structural Dynamics, and Materials Conference*, AIAA, Hilton Head, SC, 1994.
[13] T. Hasselman, G. Wathugala, Top–down vs, bottom–up uncertainty quantification for validation of a mechanical joint model, *Proceedings of the 23rd International Modal Analysis Conference*, Orlando, FL, 2005.
[14] T. Hasselman, Uncertainty quantification in verification and validation of computational solid mechanics models—modeling, *Proceedings of the 50th AIAA/ASME/ASCE/AHS/ASC Structures, Structural Dynamics, and Materials Conference*, Palm Springs, CA, 2009.
[15] L. Hinke, B.R. Mace, N.S. Ferguson, Uncertainty quantification and CMS: free and fixed-interface methodologies, *Proceedings of the 25th International Modal Analysis Conference*, Orlando, FL, 2007.
[16] R.R. Craig, M.C.C. Bampton, Coupling of substructures for dynamic analysis, *AIAA Journal* 6 (7) (1968) 1313–1319.
[17] D. de Klerk, S.N. Voormeeren, Uncertainty propagation in experimental dynamic substructuring, *Proceedings of the 26th International Modal Analysis Conference*, Orlando, FL, 2008.
[18] V. Babuska, D. Carter, S. Lane, Uncertainty propagation and substructure synthesis using LFTs, *Proceedings of the 47th AIAA Structures, Structural Dynamics, and Materials Conference*, Newport, RI, 2006.
[19] B.R. Mace, P.J. Shorter, A local modal/perturbational method for estimating frequency response statistics of built-up structures with uncertain properties, *Journal of Sound and Vibration* 242 (5) (2001) 793–811.
[20] T. Hasselman, Quantification of uncertainty in structural dynamic models, *Journal of Aerospace Engineering* 14 (4) (2001) 158–165.
[21] D.C. Kammer, Test-analysis model development using an exact modal reduction, *International Journal of Analytical and Experimental Modal Analysis* 2 (4) (1987) 174–179.
[22] W.H. Steeb, *Matrix Calculus and Kronecker Product with Applications and C++ Programs*, World Scientific, Singapore, 1997.
[23] J.R. Magnus, H. Neudecker, *Matrix Differential Calculus with Applications in Statistics and Econometrics*, John Wiley & Sons, 1988.
[24] C. Soize, Maximum entropy approach for modeling random uncertainties in transient elastodynamics, *Journal of the Acoustic Society of America* 109 (5) (2001) 1979–1996.